Fluid Dynamics & Materials Processing FDMP, vol.16, no.1, pp.41-53, 2020

Numerical Investigation of the Deposition Characteristics of Snow on the Bogie of a High-Speed Train

Lu Cai[1], Zhen Lou[1], Nan Liu[2], Chao An[2] and Jiye Zhang[1,*]

Abstract: To investigate the deposition distribution of snow particles in the bogie surfaces of a high-speed train, a snow particle deposition model, based on the critical capture velocity and the critical shear velocity, was elaborated. Simulations based on the unsteady Reynolds-Averaged Navier-Stokes (RANS) approach coupled with Discrete Phase Model (DPM) were used to analyze the motion of snow particles. The results show that the cross beam of the bogie frame, the anti-snake damper, the intermediate brake clamps in the rear wheels, the traction rod and the anti-rolling torsion bar are prone to accumulate snow. The accumulation mass relating to the vertical surface in the rear region, horizontal surface in the front region and the corner area of the bogie is high. The average snow accumulation mass for each component ordered from high to low is as follow: traction rod, frame, bolster, brake clamp 2, anti-rolling torsion bar, brake clamp 1, transverse damper, axle box 2, axle box 1, air spring, anti-snake damper, tread cleaning device. The snow accumulation mass on the front components of the bogie is more significant than that relating to the rear components. Particularly, the average snow accumulation mass of rear brake clamp 2 and axle box 2 is about twice as high as that of the front brake clamp 1 and axle box 1.

Keywords: High-speed train, bogie, discrete phase model, snow drift, snow accumulation.

1 Introduction

When a high-speed train runs on a snow-covered railway, the snow particle on trackside is stirred up by the slipstream of the running train, which will form a snow stream around the train and deposit on the bogie surface. The heat radiated by the motors and gearbox of the high-speed train will melt the snow into the water, which can be turned into ice in a low-temperature environment. When the snow or ice accumulating on the bogie reached a level, it will hinder the movement of the suspension system, squeeze or damage the components of the bogie, and the effectiveness of the damping system and braking device will be affected [Kloow (2011)]. To solve this issue, several studies have been undertaken in the past decades. Shishido et al. [Shishido, Nakade, Ido et al. (2007)] studied the effects of the deflector on the side of the skirt plate on snow accumulation of

[1] State Key Laboratory of Traction Power, Southwest Jiaotong University, Chengdu, China.

[2] CRRC Tangshan Co., Ltd., Tangshan, China.

[*] Corresponding Author: Jiye Zhang. Email: jyzhang@home.swjtu.edu.cn.

Received: 22 June 2019; Accepted: 07 August 2019.

bogie in the snowfall wind tunnel. Ido et al. [Ido, Saitou, Nakade et al. (2008)] studied the effects of triangular diamond spoiler on snow accumulation of the bogie region in the low-temperature wind tunnel. Most of the research about snow disasters for a high-speed train is mainly focused on improving the line environment, increasing snow removal and deicing measures. The mechanism of snow accretion in the bogie region is rarely mentioned in literature.

At present, snowdrift researches are mostly concentrated in the field of buildings. The rapid increase of computational power and advances in computer software have enabled the computational fluid dynamics (CFD) to predict snowdrift around buildings [Beyers and Waechter (2008); Zhu, Yu, Zhao et al. (2017); Tominaga (2018)]. Different from the snow drifting in the atmospheric boundary layer, the drift of snow particles at the underneath of high-speed train is mainly caused by train induced wind. The research of Kwon et al. [Kwon and Park (2006)] shows that the wind speed caused by train can be reached 40% of the running speed at the height of 0.18 m above the track ground. The strong underbody flow of a high-speed train will detach the snow particles from the snow bed, and then carry snow particles into the bogie region. Wang et al. [Wang, Zhang, Zhang et al. (2018); Wang, Zhang, Xie et al. (2018)] studied the influence of the slope of the end wall of the bogie cabin on snow accumulation of the bogie by using the DPM, and analyzed the effects of train speed, snow particle density and size on snow accumulation. Paradot et al. [Paradot, Allain, Croué et al. (2014)] established a snow particle capture criterion for snow accumulation analysis based on the wind tunnel test data and investigated the snow accretion process on the bogie surface using DPM coupled with the grid deformation tool. Gao et al. [Wang, Gao, Zhang et al. (2018); Gao, Zhang, Xie et al. (2018)] analysed the snow distribution on the bogie by using the DPM and validated the results against the experimental data. Trenker et al. [Trenker and Payer (2006)] used DPM and user-defined boundary conditions of snow particle to analyse the accumulation rate of snow particles on train-set equipment.

In the above studies of snow-wind multi-phase flow, the treatment of snow phase can be divided into Euler method and Lagrangian method. The Lagrangian method can more intuitively simulate the motion mechanism of snow particles from the perspective of individual microscopic particles. Besides, it gives the complete information on particle impact at the surface required for sticking studies [Ei-Batsh and Haselbacher (2002)]. Therefore, this method has been chosen in the present work to study the snow particles movement due to underbody flow of high-speed train.

For the purpose of better understanding the deposition mechanism of snow particles in the bogie region, a snow particle deposition model based on the critical capture velocity and the critical shear wind speed was established to deal with the impact behavior between snow particles and bogie surface and to calculate the mass of snow accumulated on the bogie surface. The results of previous numerical studies using DPM method show good agreement with the experimental data. Thus, this method has been chosen in the present work to study the wind-snow two-phase flow in the bogie region. At the same time, the motion and deposition characteristics of snow particle on the bogie surfaces were analysed.

2 Numerical modeling

2.1 Geometric model and computational domain

When the DPM is used to simulate the movement of snow particles, it is not suitable to use scale model to simulate the wind-snow two-phase flow because of the snow particles are not suitable for the similarity criterion [Wang, Zhang, Zhang et al. (2018)]. If the three-section full-size train model is adopted, the DPM method will consume a lot of computing resources. Considering that the flow far away from the front and rear of the train and the bogie region is less affected by the upstream and the upper shape of the car body [Wang, Gao, Zhang et al. (2018); Gao, Zhang, Xie et al. (2018)], the local region of the bogie was studied in this paper in order to save the computing resources. The geometric model, as shown in Fig. 1, includes a complex trailer bogie and a simplified car body. The car body was simplified to a bogie cavity having the same side shape of the whole train and 30° inclined end surfaces. The length of the computational domain is 70 m (7 L), the top is 30 m from the ground, and the left and right side are 25 m from the centre line of the track. The inlet is 20 m from the tip of the bogie cavity, and the bottom of the bogie cover is 0.2 m from the rail top.

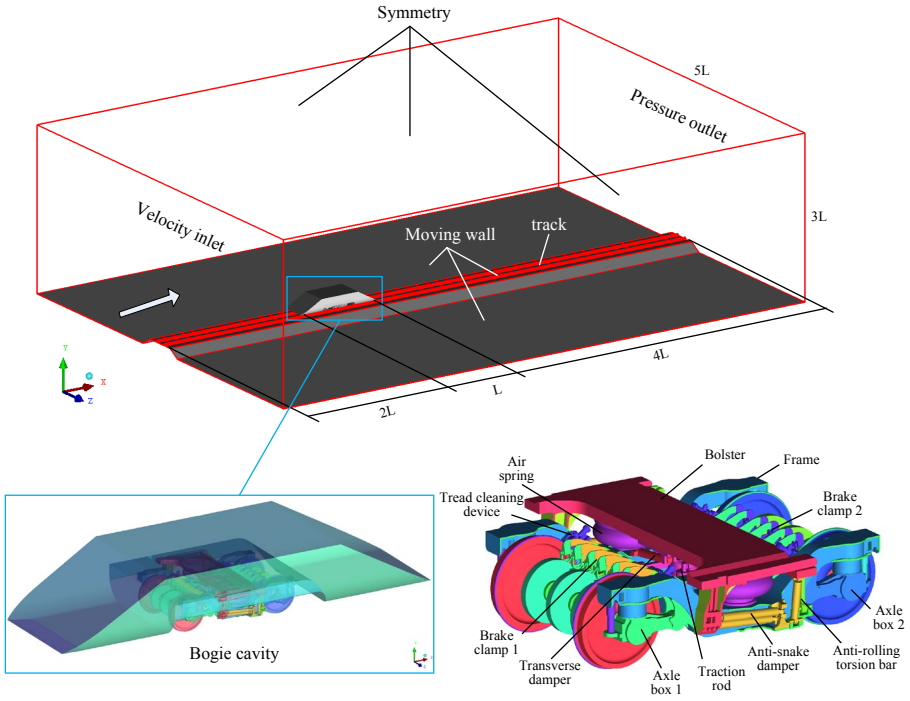

Figure 1: Geometric mode

2.2 Model for suspension of snow particles

Based on Reynolds-Averaged Navier-Stokes (RANS) equation, the Realizable $k-\varepsilon$ turbulence model [Shih, Liou, Shabbir et al. (1995)] was used to simulate the continuous phase. The wind tunnel test results [Gao, Zhang, Xie et al. (2018)] show that the

Realizable $k-\varepsilon$ model is an appropriate turbulence model for calculating the flow field in the bogie region. The trajectory of a discrete phase particle is described by integrating the force balance on the particle, which is written in a Lagrangian reference frame. The update of the velocity and displacement of each particle is determined by the collision process of the adjacent particle and the suspension process of the fluid, and the instantaneous effects of the particles on the fluid are included in the source terms which are constantly modified in the process of solving the RANS equation. Assuming that the snow particles are spherical, regardless of the collision between snow particles, the force balance equation of snow particles are presented as follows:

$$m_p \frac{d\vec{u}_p}{dt} = m_p \frac{\vec{u}-\vec{u}_p}{\tau_r} + m_p \frac{\vec{g}\left(\rho_p-\rho\right)}{\rho_p} + \vec{F} \tag{1}$$

where m_p is the particle mass, $\vec{u}$ is the fluid velocity, $\vec{u}_p$ is the particle velocity, μ is the hydrodynamic viscosity, ρ is the fluid density, ρ_p is the density of particle, d_p is the particle diameter, $\vec{F}$ is an additional force, $m_p \frac{\vec{u}-\vec{u}_p}{\tau_r}$ is the drag force, and τ_r is the particle relaxation time, calculated by:

$$\begin{cases} \tau_r = \dfrac{\rho_p d_p^2}{18\mu} \dfrac{24}{C_D \,\mathrm{Re}} \\ \mathrm{Re} = \dfrac{\rho d_p \left|\vec{u}_p - \vec{u}\right|}{\mu} \end{cases} \tag{2}$$

The particle uses a smooth sphere model [Morsi and Alexander (1972)] and the drag coefficient C_D is defined as:

$$C_D = a_1 + \frac{a_2}{\mathrm{Re}} + \frac{a_3}{\mathrm{Re}^2} \tag{3}$$

Here, a_1, a_2, and a_3 is a constant related to the range of Re numbers, see Morsi et al. [Morsi and Alexander (1972)].

Because of the numerical simulation using the wind tunnel mode, the speed of snow particle leaving the snow bed is low compared with the running speed of the train, and the initial relative speed of the snow particles is approximate the train speed. Therefore, the fixed injection surface was used to releasing snow particles into the underneath of the car body. The injector was arranged at the underneath of the bogie cavity (see Fig. 2), its height is from the bottom of the rail to the bottom of the bogie cover, and its width is the same as the train. The initial speed of the injection particles is 83.33 m/s, which equal to the running speed of the train (in the opposite direction). The snow particles were simplified to spheres with uniform diameters and density. The mass flow rate of the injector is 0.1 g/s. The snow particles were simplified to spheres with uniform diameters and density. According to some related literature [Beyers and Waechter (2008); Gao, Zhang, Xie et al. (2018)], the medium size snow particles diameter d_p is 200 μm, and

the density ρ_p is 150 kg/m^3.

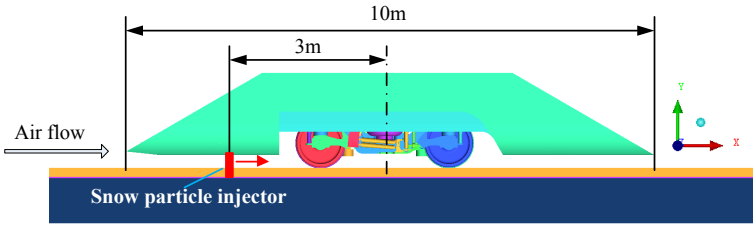

Figure 2: Arrangement of the particle injector

2.3 Snow particle deposition model

Based on the EI-Batsh particle deposition model [Ei-Batsh and Haselbacher (2002)], a snow particle deposition model using the critical capture velocity and the critical friction wind velocity was established. When the incident velocity u_{p} of snow particles is less than the critical capture velocity u_{trap}, the snow particles stick to the surface; otherwise, the snow particles rebound. If the frictional wind speed $u*$ at the particle impact point is higher than the critical friction wind speed u_{*t}, the snow particles will not be stably deposited, and the particles will be blown away. The impact results between the snow particles and the bogie surface are shown in Fig. 3. Exact material parameters with meteorological condition dependency are not available. Thus, the deposition model is parameterized with data taken from the literature. The study by Kind [Kind (1976)] showed that the critical friction wind speed of snow-bed after a period of wind erosion is 0.25 to 1.0 m/s. Considering that the running speed of the high-speed train is high, the speed of the snow particles hitting the bogie surface is relatively high, and the snow will be compacted, so u_{*t} is taken upper limit value 1.0 m/s in this paper. The experimental results of snowflakes impact with snow surface by using artificial snowflakes [Sato, Kosugi, Mochizuki et al. (2008)] show that when the vertical incident velocity V_i of the snowflake is reached $3.0 \sim 3.8$ m/s, the snowflake is completely decomposed into snow crystals and blown away. Hence, the critical capture velocity is 3.0 m/s in this paper.

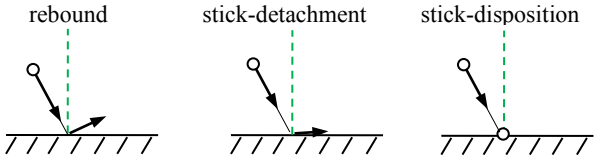

Figure 3: Results of impact between snow particles and surface

To analyze the deposit characteristics of snow particle on the bogie surface, a user-defined memories (UDM) was defined in the Fluent software to store the accumulation mass of snow on the bogie surface. The accumulation mass was defined as the mass of the particles sticking at the surface per unit area. The impact behaviour between the snow

particles and the bogie surface was realized by user-defined functions (UDF), and the calculation results of the relevant statistics on the bogie surface were stored in the UDM. The calculation processes (see in Fig. 4) are shown as follows:

(1) Calculating the friction wind velocity (u_*) at the impact point between snow particles and bogie surface and the incident velocity (u_p) of the snow particles.

(2) Judging whether the incident velocity (u_p) of the impact snow particle is less than the critical capture velocity (u_{trap}): if $u_p \le u_{trap}$, captured snow particle and waits for further judgment, otherwise, the new rebound velocity is calculated and the snow particle trajectory is activated.

(3) Determining whether the friction wind velocity (u_*) at the snow particles captured point is less than the critical friction wind velocity (u_{*t}): if $u_* \le u_{*_t}$, the snow particles are determined to be accumulated and the accumulation mass on the surface is calculated, and the trajectory of the snow particles is terminated, otherwise, the particles are cut away by the airflow. It is assumed that the velocity obtained by the snow particles cut by the airflow is equal to the friction wind velocity, and the trajectory of the snow particle is activated.

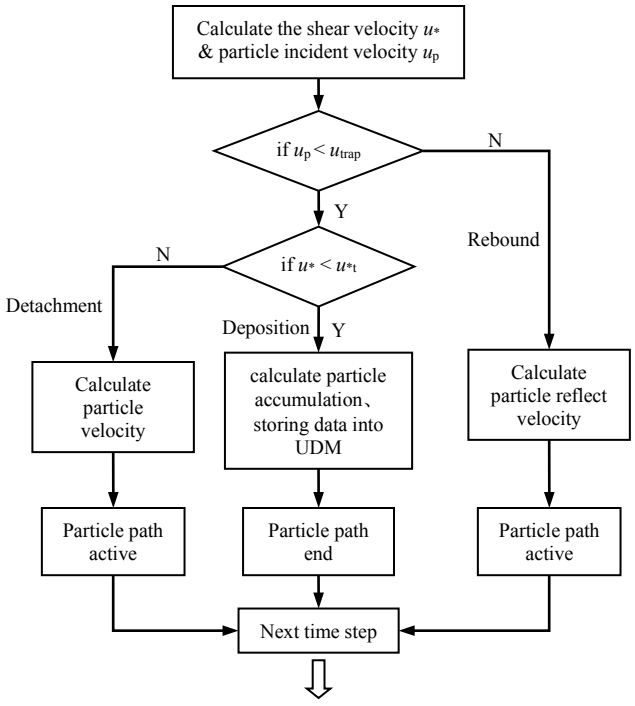

Figure 4: Flow chart of calculation

2.4 Computational mesh

The tetrahedral mesh was used for the discretization of the fluid domain, local refinement of the mesh around the simplified car body and the bogie region. The wall function was

used in the near wall region, and the boundary layer was divided into 10 layers near the wall. The mesh growth rate was 1.2, and the wall y^+ was roughly in the range of 30 to 300, most of which were less than 100 [Versteeg and Malalasekera (2007)]. Three sets of grids (coarse, medium and fine grids) with 18, 24 and 34 million cells were applied to investigate the effects of grid density, and the most suitable grid was selected for further investigations. The size change rate of the grids was about 1.2, but the size setting of the boundary layer was the same. The pressure coefficients C_p on the centerline at 0.1 m above the rail top surface were calculated in the three grids, as shown in Fig. 5. It indicates that the tendencies of C_p in the three grids are consistent with each other. Especially, medium grids have a good agreement with the fine grids. However, the result of coarse grids exhibits difference for the other two grids at 16.5<x<17.5 m for the centerline. The grid sensitivity test demonstrates that the resolution of the medium grids is adequate. Therefore, all of the cases in this paper are based on the grid sensitivity test using the medium grid. Details of the computational grid are shown in Fig. 6.

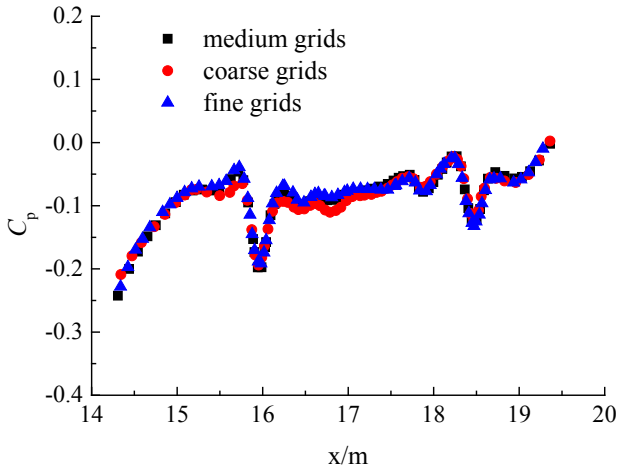

Figure 5: Pressure coefficients along the centerline under the bogie

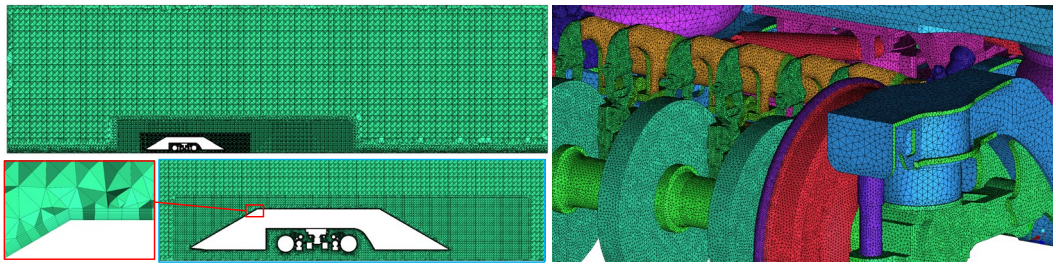

(a) (b)

Figure 6: Computational mesh (a) volume meshes in the middle section (b) surface meshes of the bogie

2.5 Numerical methodology and boundary conditions

In the present simulation, the unsteady RANS equations and the Realizable $k-\varepsilon$ turbulence model was used in the continuous phase, and the DPM was used in the snow particle phase. The steady calculation results were used to initialize the transient calculation. A time step of 1e-4 s was used for continuous phase solver, 20 iterations in each time step, and the total solution time was 1.5 s. Inject particles once at each continuous phase time step by using the non-steady particle tracking method, and DRW (Discrete Random Walk) model was selected to include the effect of turbulent dispersion on the trajectory of snow particles. Max. Number of Steps for particle trajectories was set to 5000, which satisfies the time required for particles to flow through the computational domain. The Step Length Factor λ was set to 10, which satisfies $\lambda \times N$ (N is the number of mesh cells along the flow direction of the particle advance through the domain) is approximately equal to the Max. Number of Steps.

The boundary conditions are shown in Tab. 1. The snow-wall boundary condition parameters are as follows: the capture speed is 3.0 m/s; the critical friction wind speed is 1.0 m/s; the normal rebound coefficient is 0.01; the tangential rebound coefficient is 0.2. In addition, the extreme atmospheric temperature along the Harbin-Dalian high-speed railway in China is about -30ºC [Liu and Niu (2016)]，the density and viscosity of air at -30ºC were adopted in simulation.

Table 1: Details of the boundary conditions

Boundary	Air phase boundary condition	Parameter setting	Snow phase boundary condition
Inlet	Velocity inlet	X=83.33 m/s Turbulence Intensity: 1% Turbulence Viscosity Ratio: 10%	escape
Outlet	Pressure outlet	0 Pa	escape
Side-wall & up-wall	Symmetry	-	-
Tracks & ground	Moving wall: transition	83.33 m/s	escape
Wheels	Moving wall: rotation	181.9 rad/s	reflect
Bogie (except wheels)	No-slip wall	-	UDF
Bogie cavity	No-slip wall	-	UDF

3 Results and discussion

3.1 Snow drifting characteristic in the bogie region

Fig. 7 shows the velocity vector of snow particles entering the bogie region. The snow particles in the upper layer of the suspended snow particles underneath the bogie are decelerated under the action of the negative pressure gradient in the bogie region and turn upward from the rear of the two wheels into the internal area of the bogie. Meanwhile,

the snow particles in the lower layers of the suspended snow particles below the bogie will be carried away directly by the airflow and will not enter the bogie region. Fig. 8 shows the distribution of snow particles in the bogie region at the time of 1.0 s, where snow particles colored by particle residence time. The residence time of the most snow particles in the bogie region is less than 0.6 s, indicating that the movement of snow particles in the bogie region reaches a stable state after the computation time of 0.6 s.

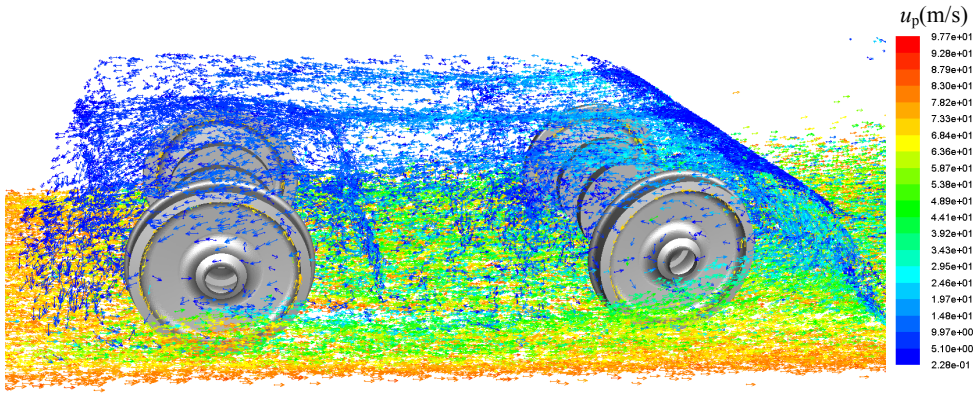

Figure 7: The velocity vector of snow particles in the bogie region at t=0.6 s

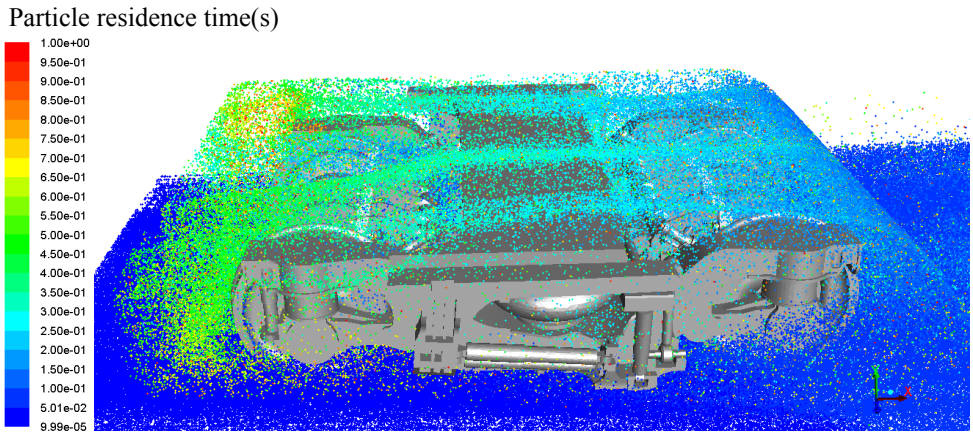

Figure 8: Distribution of snow particles in the bogie region at t=1.0 s

3.2 Deposition characteristics of snow particle on the bogie surface

Fig. 9 shows the distribution of accumulation mass of snow particles on the bogie surface within 1.5 seconds at the incoming flow speed of 83.33 m/s. The accumulation mass of snow particles on the component surfaces which directly impacted by the incoming flow and the upward overturning air flow is high, such as the front surfaces of the cross beam of the bogie frame and the rear surface of the bogie in the rear wheels (axle 2) region. Among them, the accumulation mass of snow particles of the rear side of the bolster and the traction rod, the middle brake clamp of the rear wheels is more than 0.1 g/m^2. On the

side of the anti-snake damper and the axle box suspension of the rear wheels, its accumulation mass of snow particles is more than 0.05 g/m^2. Overall, the upper area of the frame, the anti-snake damper, the middle brake clamp of the rear wheels, the traction rod and the anti-roll torsion bar are easy to accumulate snow particles. These components are the critical suspension and braking components, which can significantly influence the safety of the train.

The snow accretion on the actual bogie of a high-speed train is shown in Fig. 10. The disposition characteristics of the snow particles on the bogie region in the numerical simulation are similar to the case that high-speed train is running in winter in Fig. 10. It is observed that the severe snow accretion exists in the middle region of the bogie and the first suspension device. The snow distributions on the bogie show good agreement in simulation and actual. It should be noted that the simulation results in this paper only reflect the snow deposition characteristics of the initial surface of the bogie. In reality, as the snow on the bogie surface increase, the wall of the bogie region will change.

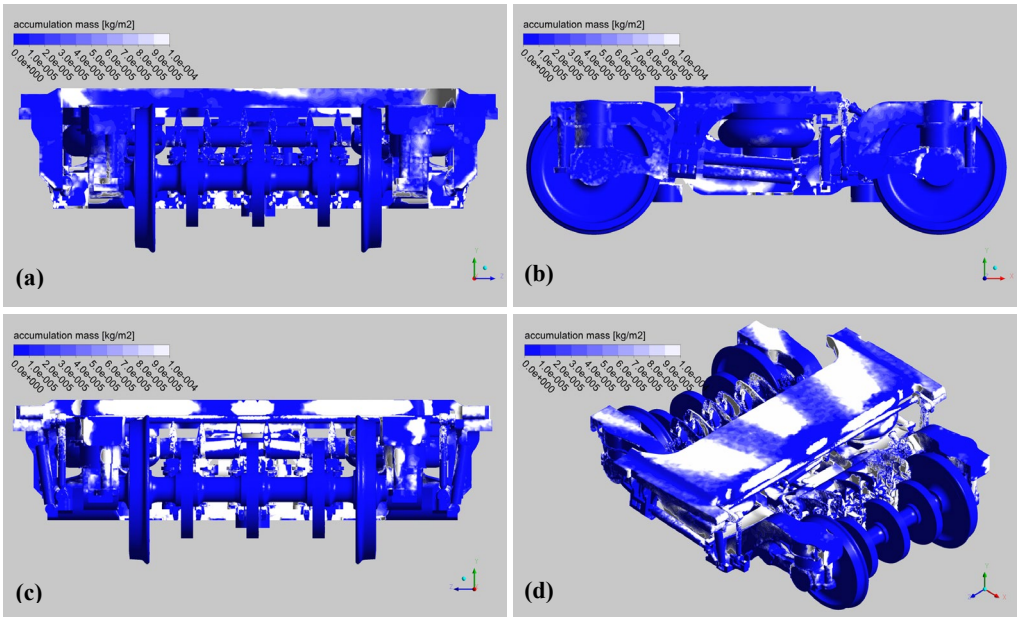

Figure 9: Distribution of snow accumulation mass on the bogie surface (a) front view (b) side view (c) back view (d) axonometric projection

(a) (b)

Figure 10: Snow accretion on the bogie of high-speed train (a) now accretion exists in the middle region of the bogie (b) snow accretion exists in the first suspension device

In order to evaluate the efficiency of snow accretion on each component, the amount of snow accumulation on each component was calculated by integrating the snow accumulation per unit area with the surface area, and then divides by surface areas of component to get the average value of snow accumulation on component. As shown in Fig. 11(a), **the average accumulation mass of snow** (total accumulation mass/total area of component) on each component from high to low is traction rod, frame, brake clamp 2, bolster, anti-roll bar, brake clamp 1, transverse damper, axle box suspension 2, air spring, anti-snake damper, axle box suspension 1, tread cleaning device. Among them, **the average accumulation mass of snow** of traction rod, frame, clamp 2 and bolster is about twice as high as that of other components. Furthermore, it has been found that **the average accumulation mass of snow** on the front components of the bogie is larger than that on the rear components. Particularly, the average snow accumulation of rear brake clamp 2 and axle box 2 is about twice as high as that of front brake clamp 1 and axle box 1.

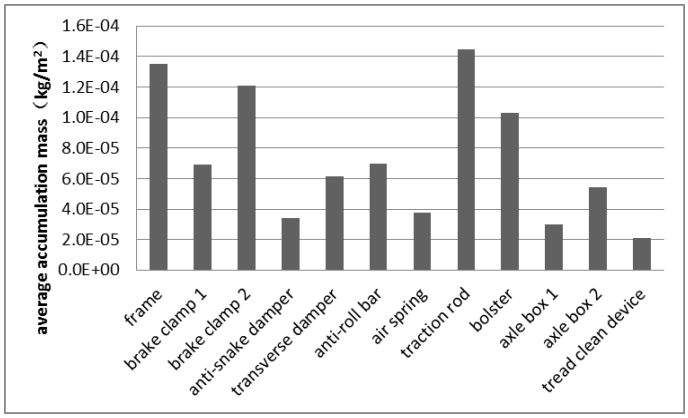

Figure 11: Average accumulation mass of snow on each component

4 Discussion and conclusions

(1) The average accumulation mass of each component from high to low is traction rod, frame, brake clamp 2, bolster, anti-roll bar, brake clamp 1, transverse damper, axle box

suspension 2, air spring, anti-snake damper, axle box suspension 1, tread cleaning device. Among them, the average snow accumulation mass of traction rod, frame, clamp 2 and bolster is about twice as high as that of other components. The snow accumulation mass at the front components of the bogie is larger than that at the rear components. Particularly, the average snow accumulation mass of rear brake clamp 2 and axle box 2 is higher two times than that of the front brake clamp 1 and axle box 1.

(2) The cross beam of the bogie frame, the anti-snake damper, the middle brake clamp of the rear wheels, the traction rod and the anti-roll torsion bar, are the components which the snow particles are easy to accumulate. The accumulation mass of vertical surface in the rear region, horizontal surface in the front region and the corner region of the bogie is high. The snow will begin to develop in the middle region of the bogie, and the accumulation speed of snow particle in the rear components is faster than that in the front components.

Acknowledgement: This work was supported by the National Key Research and Development Program of China [Grant No. 2016YFB1200402]. The authors acknowledge the computing resources provided by the Laboratory for Rail Transportation.

Conflicts of Interest: The authors declare that they have no conflicts of interest to report regarding the present study.

References

Beyers, M.; Waechter, B. (2008): Modeling transient snowdrift development around complex three-dimensional structures. *Journal of Wind Engineering & Industrial Aerodynamics*, vol. 96, pp. 1603-1615.

Ei-Batsh, H.; Haselbacher, H. (2002): Numerical investigation of the effect of ash particle deposition on the flow field through turbine cascades. *ASME Turbo Expo: Power for Land, Sea, and Air, Volume 5: Turbo Expo 2002, Part A and B*, pp. 1035-1043.

Gao, G. J.; Zhang, Y.; Xie, F.; Zhang, J.; He, K. et al. (2019): Numerical study on the anti-snow performance of deflectors in the bogie region of a high-speed train using the discrete phase model. *Proceedings of the Institution of Mechanical Engineers, Part F: Journal of Rail & Rapid Transit*, vol. 233, no. 2, pp. 141-159.

Ido, A.; Saitou, S.; Nakade, K.; Iikura, S. (2008): Study on under-floor flow to reduce ballast flying phenomena. *Proceedings of the Word congress on Rail Research*.

Kind, R. J. (1976): A critical examination of the requirements for model simulation of wind-induced erosion/deposition phenomena such as snow drifting. *Atmospheric Environment*, vol. 10, no. 3, pp. 219-227.

Kloow, L. (2011): High-speed train operation in winter climate. *KTH Railway Group and Transrail*.

Kwon, H. B.; Park, C. S. (2006): An experimental study on the relationship between ballast flying phenomenon and strong wind under high speed train. *Proceedings of the Word Congress on Rail Research*.

Liu, H.; Niu, F. (2016): Effect of structures and sunny-shady slopes on thermal

characteristics of subgrade along the Harbin-Dalian passenger dedicated line in Northeast China. *Cold Regions Science and Technology*, vol. 123, pp. 14-21.

Morsi, S. A.; Alexander, A. J. (1972): An investigation of particle trajectories in two-phase systems. *Journal of Fluid Mechanics*, vol. 55, pp. 193-208.

Paradot, N.; Allain, E.; Croué, R.; Delacasa, X.; Pauline, J. (2014): Development of a numerical modeling of snow accumulation on a high speed train. *International Conference on Railway Technology: Research, Development and Maintenance*.

Sato, T.; Kosugi, K.; Mochizuki, S.; Memoto, M. (2008): Wind speed dependences of fracture and accumulation of snowflakes on snow surface. *Cold Regions Science & Technology*, vol. 51, pp. 229-239.

Shih, T. H.; Liou, W.; Shabbir, A.; Yang, Z.; Zhu, J. (1995): A new $k-\varepsilon$ eddy-viscosity model for high Reynolds number turbulent flows-model development and validation. *Computers Fluids*, vol. 2, no. 3, pp. 227-238.

Shishido, M.; Nakade, K.; Ido, A.; Iikura, S; Kamata, Y. et al. (2007): Development of, deflector to decrease, snow-accretion to the bogie of train. *Preprints of the Annual Conference: Japanese Society of Snow and Ice*.

Tominaga, Y. (2018): Computational fluid dynamics simulation of snowdrift around buildings: past achievement and future perspectives. *Cold Regions Science & Technology*, vol. 150, pp. 2-14.

Trenker, M.; Payer, W. (2006): Investigation of snow particle transportation and accretion on trains. *24th AIAA Applied Aerodynamics Conference, AIAA 2006-3648*.

Versteeg, H. K.; Malalasekera, W. (2007): *An Introduction to Computational Fluid Dynamics: the Finite Volume Method*. Pearson Education Limited.

Wang, J. B.; Gao, G. J.; Zhang, Y.; He, K.; Zhang, J. (2018): Anti-snow performance of snow shields designed for brake calipers of a high-speed train. *Proceedings of the Institution of Mechanical Engineers, Part F: Journal of Rail & Rapid Transit*. vol. 233, no. 2, pp. 121-140.

Wang, J. B.; Zhang, J.; Xie, F.; Zhang, Y.; Gao, G. J. (2018): A study of snow accumulating on the bogie and the effects of deflectors on the de-icing performance in the bogie region of a high-speed train. *Cold Regions Science & Technology*, vol. 148, pp. 121-130.

Wang, J. B.; Zhang, J.; Zhang, Y.; Xie, F.; Krajnovic, S. et al. (2018): Impact of bogie cavity shapes and operational environment on snow accumulating on the bogies of high-speed trains. *Journal of Wind Engineering & Industrial Aerodynamics*, vol. 176, pp. 211-224.

Zhu, F.; Yu, Z. X.; Zhao, L.; Xue, M. Q.; Zhao, S. C. (2017): Adaptive-mesh method using RBF interpolation: a time-marching analysis of steady snow drifting on stepped flat roofs. *Journal of Wind Engineering & Industrial Aerodynamics*, vol. 171, pp. 1-11.